

C₁₂ Helices in Long Hybrid ($\alpha\gamma$)_n Peptides Composed Entirely of Unconstrained Residues with Proteinogenic Side Chains

Rajesh Sonti,^{‡,†,||} Bhimareddy Dinesh,^{†,||} Krishnayan Basuroy,[§] Srinivasarao Raghothama,[‡] Narayanaswamy Shamala,[§] and Padmanabhan Balaram^{*,†}

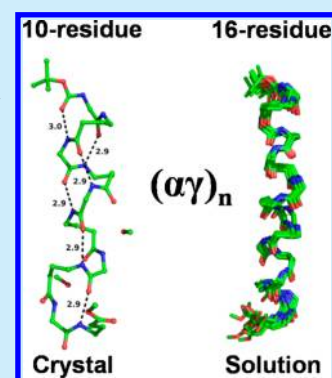
[†]Molecular Biophysics Unit, Indian Institute of Science, Bangalore, India, 560012

[‡]NMR Research Centre, Indian Institute of Science, Bangalore, India, 560012

[§]Department of Physics, Indian Institute of Science, Bangalore, India, 560012

S Supporting Information

ABSTRACT: Unconstrained γ^4 amino acid residues derived by homologation of proteinogenic amino acids facilitate helical folding in hybrid ($\alpha\gamma$)_n sequences. The C₁₂ helical conformation for the decapeptide, Boc-[Leu- γ^4 (R)Val]₅-OMe, is established in crystals by X-ray diffraction. A regular C₁₂ helix is demonstrated by NMR studies of the 18 residue peptide, Boc-[Leu- γ^4 (R)Val]₉-OMe, and a designed 16 residue ($\alpha\gamma$)_n peptide, incorporating variable side chains. Unconstrained ($\alpha\gamma$)_n peptides show an unexpectedly high propensity for helical folding in long polypeptide sequences.



Homologated amino acid residues in which additional methylene groups have been inserted into the backbone have shown a surprising tendency to promote folded polypeptide conformations, despite the introduction of additional degrees of torsional freedom.¹ The foldability of γ -peptides derived from homologues of the proteinogenic α -amino acids was first reported, in the studies of short peptides in organic solvents, by Seebach² and Hanessian³ in the 1990s. These observations coincided with the discovery by Gellman that oligo- β -peptides form novel helical structures, unambiguously characterized by single crystal X-ray diffraction.⁴ The rapidly advancing field of foldamers,^{1b,5} which focuses on non- α -amino acid backbones, has stimulated a great deal of interest in the structural and functional properties of β - and γ -peptides.^{1a,6} The definitive characterization of the precise conformational features of β - and γ -peptides has been greatly facilitated by the use of conformationally constrained (“preorganized”) residues, which promote folded structures in solution and enhance peptide crystallizability.⁷ Recent work on γ -peptide sequences containing exclusively unconstrained residues derived from the protein amino acids have established a very high propensity for the formation of folded helical structures,⁸ specifically the C₁₄ helix in oligomeric γ -peptide sequences.⁹

Hybrid polypeptides, which contain α -, β -, and γ -residues, provide a means of expanding the structure space of synthetic polypeptides, a desirable goal in the design of peptidomimetics. Regular hybrid sequences ($\alpha\beta$)_n, ($\alpha\gamma$)_n, ($\beta\gamma$)_n, etc. afford an opportunity to characterize helical structures, which are

expanded analogues of the 3₁₀ and α -helical structures in α -polypeptides and proteins.¹⁰ Thus far, definitive characterization of hybrid helical structures has been achieved in designed peptides containing conformationally constrained residues, which are anticipated to promote local folding. For example, the C₁₂ helix in $\alpha\gamma$ _n sequences has been established in crystals of (U γ V)_n (U = Aib; γ V = γ^4 (R)Val) sequences ranging in length up to 16 residues.¹¹ Figure 1a illustrates the conformation in crystals of Boc-(U γ V)₅-OMe in which the hydrogen bonds of a successive C₁₂ (4 \rightarrow 1 CO_i---HN_{i+3}) stabilize the folded backbone resulting in an expanded analogue of the 3₁₀ helix. C₁₂ helices have also been characterized in Aib- γ^4 Phe sequences,^{8,12} Gabapentin (Gpn) containing sequences,¹³ and multiply substituted preorganized residues.¹⁴ The $\beta\gamma$ C₁₃ helix, which is a backbone expanded analogue of the α -helix, has recently been described in sequences containing constrained β - and γ -residues.^{7c,13d} The intriguing observation of two successive C₁₂ hydrogen bonded $\alpha\gamma$ turns (incipient C₁₂ helix) in short unconstrained $\alpha\gamma$ peptides,¹⁵ together with the observation that γ -peptides of the type (γ Val)_n, (γ Leu)_n, and (γ Ile)_n (n = 4–10) yield C₁₄ helices,⁹ suggested a high intrinsic propensity of γ^4 (R) substituted residues to adopt locally folded *gauche* (g⁺) conformations about the C γ –C β (θ_1) and C β –C α (θ_2) bonds. Encouraged by these results, we examined the possibility of designing hybrid sequences composed entirely of α - and γ -residues varying the side chains present, in order to

Received: January 28, 2014

Published: March 3, 2014

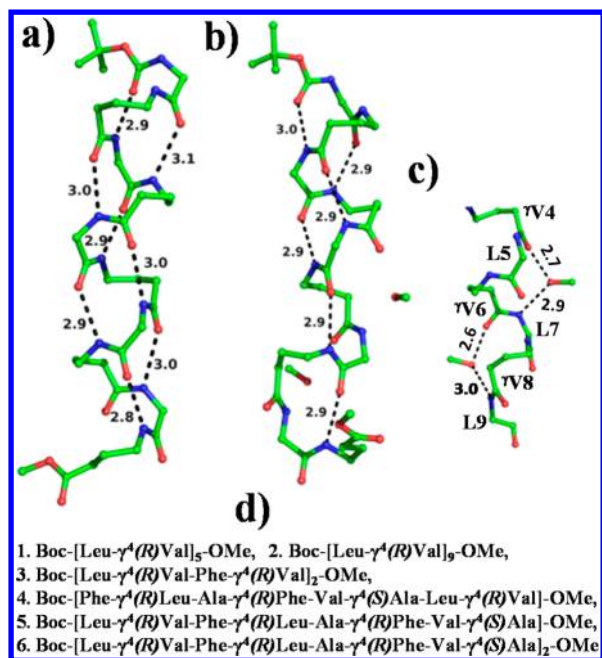


Figure 1. Molecular conformation in crystals of (a) Boc-[Aib- $\gamma^4(R)$ Val]₅-OMe¹¹ and (b) Boc-[Leu- $\gamma^4(R)$ Val]₅-OMe(1). Note the presence of two methanol molecules disrupting backbone hydrogen bonding. (c) Solvation of the backbone atoms of peptide 1 is shown. N...O (O...O) distances (Å) are indicated as broken lines. (d) Sequences of peptides studied.

assess their ability to fold into stable helices. The growing interest in the design of helical peptidomimetics,^{6a,16} for disrupting protein–protein interactions,¹⁷ provides a strong rationale for the detailed analysis of secondary structures in hybrid polypeptides containing amino acids with proteinogenic side chains. This report provides a definitive characterization of long C₁₂ helices in both the solid state and solution in $\alpha\gamma_n$ sequences containing exclusively conformationally *unconstrained* residues, derived from proteinogenic amino acids. All γ -residues are derived by homologation of the corresponding L-(S)- α amino acids as specified by the Cahn–Ingold–Prelog convention. For Val/Leu/Phe, homologation results in the R configuration, while the specified configuration for Ala is S.^{1a} The choice of apolar hydrocarbon side chains facilitates dissolution in organic solvents. Of the six sequences examined, diffraction quality single crystals were obtained, thus far, only for Boc-[Leu- $\gamma^4(R)$ Val]₅-OMe (1). X-ray diffraction data are summarized in Supplementary Table ST1, and coordinates are deposited in the CCDC database (922799). Figure 1b shows a view of the molecular conformation of 1 in crystals. Supplementary Tables ST2 and ST3 list relevant backbone torsional angles and hydrogen bond parameters.

Peptide 1 folds into a right handed $\alpha\gamma$ C₁₂ helix stabilized by six intramolecular 4→1 hydrogen bonds. Solvation of the backbone at two potential hydrogen bonding sites by methanol results in the disruption of two of the anticipated 4→1 hydrogen bonds in an ideal helix. Figure 1c shows a view of the solvent invasion of the helix backbone, a feature that has also been observed in helices formed in α -peptide crystals.¹⁸ The average values of the backbone torsional angles (deg) at both α (ϕ , ψ) and γ (ϕ , θ_1 , θ_2 , and ψ) residues for the C₁₂ helix are as follows: α , -79 ± 14.5 , -23.2 ± 13.0 ; γ , -115.8 ± 10.1 , 54.4 ± 7.0 , 65.7 ± 2.9 , -134.5 ± 10.8 . These values correspond very closely to that determined earlier for Boc-[Aib- $\gamma^4(R)$ Val]₅-

OMe,^{11a} clearly demonstrating that, despite replacement of the conformationally constrained Aib residue by the unconstrained Leu residue, a stable C₁₂ helix is indeed formed.

Persistence of the C₁₂ helix in the unconstrained ($\alpha\gamma$)_n sequence is demonstrated by the solvent dependence of NH chemical shifts in CDCl₃/DMSO mixtures. Only two NH groups assigned to the N-terminus residues Leu1 and ⁷Val2 show appreciable downfield shifts upon increasing DMSO concentration, indicative of their solvent exposure. The remaining 8 NH groups show little or no dependence of chemical shifts (Supplementary Figure S4b), suggesting that the 8 intramolecular C=O...HN hydrogen bonds anticipated in the C₁₂ helix are indeed observed in solution. The partial ROESY spectrum shown in Figure 2 establishes the presence of NH_i↔

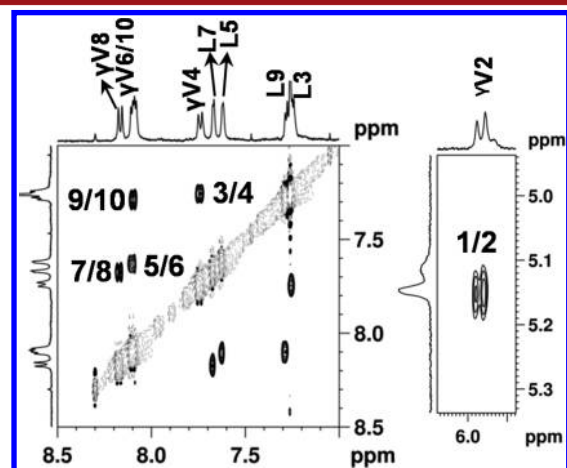


Figure 2. Partial ROESY spectrum in CDCl₃ of Boc-[Leu- $\gamma^4(R)$ Val]₅-OMe highlighting the d_{NN} NOEs.

NH_{i+1} (d_{NN}) NOEs at all five α -residues. The d_{NN} distance of approximately 3.6 Å across γ -residues results in unobservable NOEs, precluding a reliable structure calculation using experimental distance constraints. Encouraged by the evidence for a well folded structure in peptide 1, we examined the 18 residue sequence, Boc-[Leu- $\gamma^4(R)$ Val]₉-OMe (2). Figure 3a illustrates well dispersed amide NH resonances in the 18 residue peptide. Sequence specific assignments could be derived for residues 1–10, while resonance overlap precluded complete assignment of the C-terminus residues. The solvent titration curves shown in Figure 3b establish that, as in the case of peptide 1, only the NH resonances of the two residues at the N-terminus show a significant solvent dependence. These results suggest that lengthening of the hybrid $\alpha\gamma$ sequence from 10 to 18 residues results in a propagation of the folded structure over the entire length of the polypeptide chain. Local helical conformations at the α -residues are also evident in the observation of sequential d_{NN} NOEs (Figure 3c). Stimulated by the intrinsic ability of the unconstrained $\alpha\gamma$ sequences to form well folded helical structures in solution, we turned to sequences with greater side chain variability in order to enhance the chemical shift dispersion of C ^{α} H and C ^{γ} H resonances, which should enable determination of multiple distance constraints, permitting calculation of structures from solution NMR data.¹⁴ Examination of NMR data for octapeptides 3, 4, and 5 immediately revealed that enhanced chemical shift dispersion was indeed observed, facilitating the observation of additional NOEs between backbone protons of the type C ^{α} H_i↔NH_{i+1}, C ^{α} H_i↔NH_{i+2}, C ^{α} H_i↔NH_{i+3}

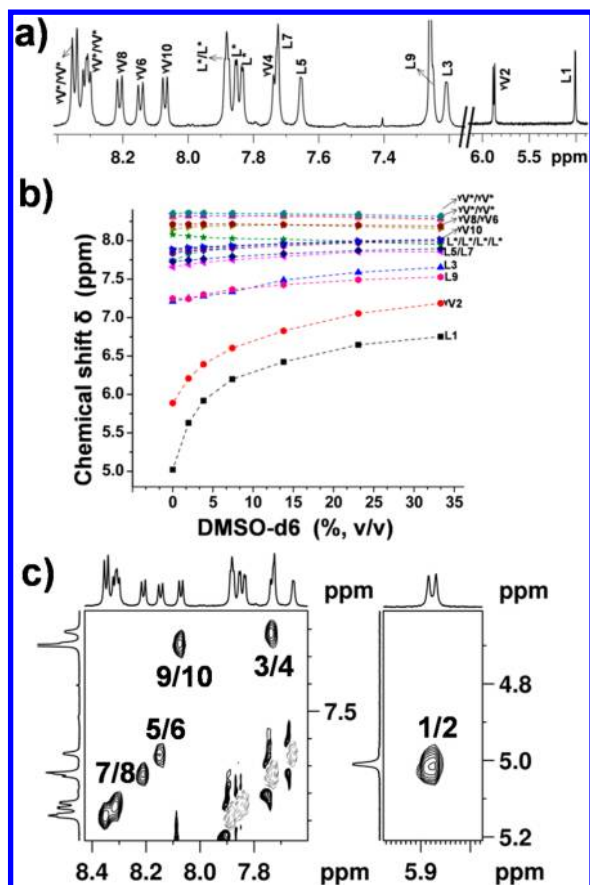


Figure 3. Peptide 2: (a) Partial ^1H NMR spectrum at 700 MHz in CDCl_3 illustrating NH resonance assignments (overlapping assignments are marked with an asterisk); (b) delineation of hydrogen bonded NH groups monitored by changes in chemical shifts of NH protons with DMSO concentration; and (c) partial ROESY spectrum highlighting the d_{NN} NOEs.

and $\text{C}^{\gamma}\text{H}$: $\text{C}^{\gamma}\text{H}_i \leftrightarrow \text{NH}_{i+1}$, $\text{C}^{\gamma}\text{H}_i \leftrightarrow \text{NH}_{i+2}$, $\text{C}^{\gamma}\text{H}_i \leftrightarrow \text{C}^{\alpha}\text{H}_{i+2}$, $\text{C}^{\gamma}\text{H}_i \leftrightarrow \text{C}^{\beta}\text{H}_{i+2}$. The results of the NMR analysis of peptides 3–5 are provided as Supporting Information (S5–S14 and ST6–ST13). Figure 4 shows the results of NMR studies on the 16 residue peptide Boc-[Leu- $\gamma^4(\text{R})$ Val-Phe- $\gamma^4(\text{R})$ Leu-Ala- $\gamma^4(\text{R})$ Phe-Val- $\gamma^4(\text{S})$ Ala] $_2$ -OMe (6). In this sequence four different kinds of α - and γ -residues have been used and an extremely well dispersed ^1H NMR spectrum was obtained at 700 MHz, permitting sequence specific assignments. Figure 4a shows the dispersion of amide NH resonances, and Figure 4b summarizes the dependence of chemical shifts in CDCl_3 /DMSO solvent titration experiments. Only two N-terminus NH resonances exhibit behavior characteristic of solvent exposed NH groups establishing the involvement of the remaining 14 NH groups in intramolecular hydrogen bonds. The sequential d_{NN} connectivities at the α -residues are illustrated in Supplementary Figure S15, while Figure 4c and 4d show nonsequential backbone proton NOEs characteristic of an $\alpha\gamma$ C_{12} helix. The key NOEs which provide important constraints for distance geometry calculations are as follows: $\text{NH}_{\alpha i} \leftrightarrow \text{NH}_{\gamma i+1}$, $\text{C}^{\alpha}\text{H}_i \leftrightarrow \text{NH}_{i+1}$, $\text{C}^{\alpha}\text{H}_i \leftrightarrow \text{NH}_{i+2}$, $\text{C}^{\alpha}\text{H}_i \leftrightarrow \text{NH}_{i+3}$, $\text{C}^{\gamma}\text{H}_i \leftrightarrow \text{NH}_{i+1}$, $\text{C}^{\gamma}\text{H}_i \leftrightarrow \text{NH}_{i+2}$, and $\text{C}^{\gamma}\text{H}_i \leftrightarrow \text{C}^{\alpha}\text{H}_{i+2}$. Using a set of 57 distance constraints and 16 torsional angle constraints at the α ($^3J_{\text{C}^{\alpha}\text{H}-\text{NH}}$, 2.5–3.5 Hz) and γ ($^3J_{\text{C}^{\gamma}\text{H}-\text{NH}}$, 8.6–10.5 Hz) residues, an NMR structure calculation yielded the family of structures shown in Figure 5a. The measured N–O distances

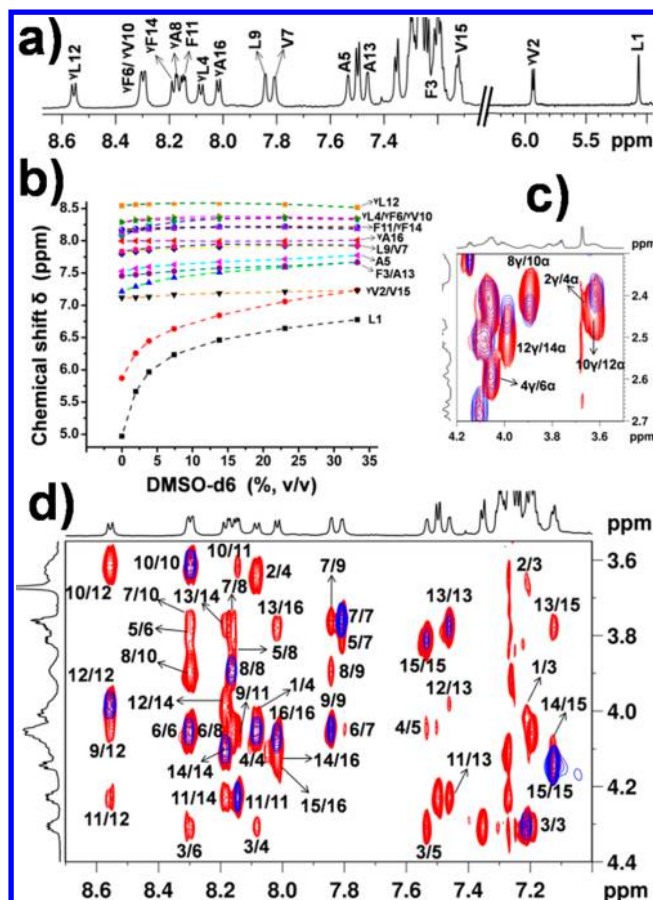


Figure 4. Peptide 6: (a) Partial ^1H NMR spectrum at 700 MHz in CDCl_3 highlighting the dispersion of NH resonances. (b) Change in NH chemical shifts with DMSO concentration in a CDCl_3 -DMSO mixture. (c,d) Partial overlay of TOCSY (blue), ROESY (red) spectra highlighting $\text{C}^{\gamma}\text{H}_i \leftrightarrow \text{C}^{\alpha}\text{H}_{i+2}$ and $\text{C}^{\gamma}\text{H}_i/\text{C}^{\alpha}\text{H}_i \leftrightarrow \text{NH}$ NOEs.

corresponding to 4 \rightarrow 1 CO---HN (C_{12}) hydrogen bonds in the NMR derived structure are 3.2–3.6 Å. A feature of the $\alpha\gamma$ C_{12} helix is the large number of nonsequential backbone interproton distances, which fall within the NOE observable limits. These diagnostic distances involving the $\text{C}^{\alpha}\text{H}_i/\text{C}^{\gamma}\text{H}_i$ protons are schematically illustrated in Figure 5b and 5c. The large number of restraints derived from backbone proton NOEs provides a robust structural characterization of the $\alpha\gamma$ C_{12} helix in solution.

The results presented above describe the crystallographic characterization of the longest C_{12} helix in an $\alpha\gamma$ hybrid peptide sequence composed entirely of unconstrained residues reported thus far. The remarkable stability of the $\alpha\gamma$ C_{12} helix even in the absence of helix nucleating, “preorganized” residues is established by the NMR structure determination of the continuous helical conformation in a 16 residue ($\alpha\gamma$) $_n$ peptide (6). Taken together, with a previously reported characterization of C_{14} helices in unconstrained γ_n sequences,⁹ the results establish a very high propensity of γ^4 residues derived by homologation of proteinogenic amino acids to facilitate helical folding in oligopeptide sequences. These observations should promote the rational design of protein mimics with hybrid peptide backbones.¹⁹

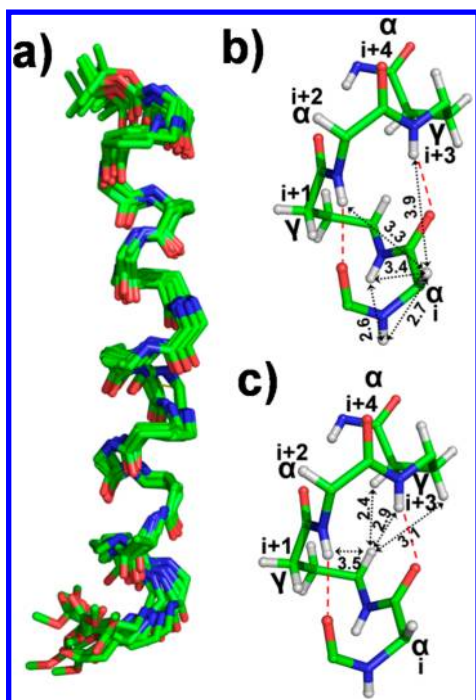


Figure 5. (a) Backbone superposition of 10 NMR determined structures of peptide 6. (b, c) Short interproton distances (Å) shown as broken lines with double edged arrows in the fragment (1–5 residues) of peptide 1 arising from (b) $C^{\alpha}H/NH$ pairs at the α -residue and (c) $C^{\gamma}H/NH$ pairs at the γ -residue. Hydrogen bonds are shown as broken red lines.

■ ASSOCIATED CONTENT

Supporting Information

Synthetic procedure, X-ray diffraction data, NMR parameters, DMSO titration curves, relevant ROESY spectra, restraints used in structure calculation, and dihedral angles are given. This material is available free of charge via the Internet at <http://pubs.acs.org>.

■ AUTHOR INFORMATION

Corresponding Author

*E-mail: pb@mbu.iisc.ernet.in.

Author Contributions

[†]These authors contributed equally.

Notes

The authors declare no competing financial interest.

■ ACKNOWLEDGMENTS

R.S. acknowledges IISc for a fellowship. This research was supported by a DBT-IISc partnership program grant.

■ REFERENCES

- (1) (a) Seebach, D.; Beck, A. K.; Bierbaum, D. J. *Chem. Biodiversity* **2004**, *1*, 1111–1239. (b) Horne, W. S.; Gellman, S. H. *Acc. Chem. Res.* **2008**, *41*, 1399–1408.
- (2) Hintermann, T.; Gademann, K.; Jaun, B.; Seebach, D. *Helv. Chim. Acta* **1998**, *81*, 983–1002.
- (3) Hanessian, S.; Luo, X.; Schaum, R.; Michnick, S. J. *Am. Chem. Soc.* **1998**, *120*, 8569–8570.
- (4) (a) Appella, D. H.; Christianson, L. A.; Karle, I. L.; Powell, D. R.; Gellman, S. H. *J. Am. Chem. Soc.* **1996**, *118*, 13071–13072. (b) Appella, D. H.; Christianson, L. A.; Klein, D. A.; Powell, D. R.; Huang, X.

- Barchi, J. J., Jr.; Gellman, S. H. *Nature* **1997**, *387*, 381–384.
- (c) Seebach, D.; Matthews, J. L. *Chem. Commun.* **1997**, 2015–2022.
- (5) (a) Gellman, S. H. *Acc. Chem. Res.* **1998**, *31*, 173–180. (b) Goodman, C. M.; Choi, S.; Shandler, S.; DeGrado, W. F. *Nat. Chem. Biol.* **2007**, *3*, 252–262. (c) Bautista, A. D.; Craig, C. J.; Harker, E. A.; Schepartz, A. *Curr. Opin. Chem. Biol.* **2007**, *11*, 685–692. (d) Guichard, G.; Huc, I. *Chem. Commun.* **2011**, *47*, S933–S941. (e) Bouillère, F.; Thétiot-Laurent, S.; Kouklovsky, C.; Alezra, V. *Amino Acids* **2011**, *41*, 687–707. (f) Martinek, T. A.; Fulop, F. *Chem. Soc. Rev.* **2012**, *41*, 687–702.
- (6) (a) Seebach, D.; Gardiner, J. *Acc. Chem. Res.* **2008**, *41*, 1366–1375. (b) Seebach, D.; Hook, D. F.; Glättli, A. *Biopolymers* **2006**, *84*, 23–37. (c) Cheng, R. P.; Gellman, S. H.; DeGrado, W. F. *Chem. Rev.* **2001**, *101*, 3219–3232. (d) Vasudev, P. G.; Chatterjee, S.; Shamala, N.; Balam, P. *Chem. Rev.* **2010**, *111*, 657–687. (e) Baldauf, C.; Hofmann, H.-J. *Helv. Chim. Acta* **2012**, *95*, 2348–2383.
- (7) (a) Guo, L.; Zhang, W.; Guzei, I. A.; Spencer, L. C.; Gellman, S. H. *Org. Lett.* **2012**, *14*, 2582–2585. (b) Vasudev, P. G.; Chatterjee, S.; Shamala, N.; Balam, P. *Acc. Chem. Res.* **2009**, *42*, 1628–1639. (c) Guo, L.; Almeida, A. M.; Zhang, W.; Reidenbach, A. G.; Choi, S. H.; Guzei, I. A.; Gellman, S. H. *J. Am. Chem. Soc.* **2010**, *132*, 7868–7869. (d) Sawada, T.; Gellman, S. H. *J. Am. Chem. Soc.* **2011**, *133*, 7336–7339. (e) Fernandes, C.; Faure, S.; Pereira, E.; Théry, V.; Declercq, V. r.; Guillot, R. g.; Aitken, D. J. *Org. Lett.* **2010**, *12*, 3606–3609.
- (8) Jadhav, S. V.; Bandyopadhyay, A.; Gopi, H. N. *Org. Biomol. Chem.* **2013**, *11*, 509–514.
- (9) Basuroy, K.; Dinesh, B.; Reddy, M. B. M.; Chandrappa, S.; Raghothama, S.; Shamala, N.; Balam, P. *Org. Lett.* **2013**, *15*, 4866–4869.
- (10) Chatterjee, S.; Roy, R. S.; Balam, P. *J. R. Soc. Interface* **2007**, *4*, 587–606.
- (11) (a) Basuroy, K.; Dinesh, B.; Shamala, N.; Balam, P. *Angew. Chem., Int. Ed.* **2012**, *51*, 8736–8739. (b) Dinesh, B.; Vinaya, V.; Raghothama, S.; Balam, P. *Eur. J. Org. Chem.* **2013**, *2013*, 3590–3596.
- (12) Bandyopadhyay, A.; Jadhav, S. V.; Gopi, H. N. *Chem. Commun.* **2012**, *48*, 7170–7172.
- (13) (a) Chatterjee, S.; Vasudev, P. G.; Raghothama, S.; Ramakrishnan, C.; Shamala, N.; Balam, P. *J. Am. Chem. Soc.* **2009**, *131*, S956–S965. (b) Ananda, K.; Vasudev, P. G.; Sengupta, A.; Raja, K. M. P.; Shamala, N.; Balam, P. *J. Am. Chem. Soc.* **2005**, *127*, 16668–16674. (c) Chatterjee, S.; Vasudev, P. G.; Ananda, K.; Raghothama, S.; Shamala, N.; Balam, P. *J. Org. Chem.* **2008**, *73*, 6595–6606. (d) Vasudev, P. G.; Ananda, K.; Chatterjee, S.; Aravinda, S.; Shamala, N.; Balam, P. *J. Am. Chem. Soc.* **2007**, *129*, 4039–4048.
- (14) Guo, L.; Chi, Y.; Almeida, A. M.; Guzei, I. A.; Parker, B. K.; Gellman, S. H. *J. Am. Chem. Soc.* **2009**, *131*, 16018–16020.
- (15) Basuroy, K.; Dinesh, B.; Shamala, N.; Balam, P. *Angew. Chem., Int. Ed.* **2013**, *52*, 3136–3139.
- (16) Aguilar, M.-I.; Purcell, A. W.; Devi, R.; Lew, R.; Rossjohn, J.; Smith, A. I.; Perlmutter, P. *Org. Biomol. Chem.* **2007**, *5*, 2884–2890.
- (17) (a) Horne, W. S.; Price, J. L.; Gellman, S. H. *Proc. Natl. Acad. Sci. U.S.A.* **2008**, *105*, 9151–9156. (b) Bullock, B. N.; Jochim, A. L.; Arora, P. S. *J. Am. Chem. Soc.* **2011**, *133*, 14220–14223.
- (18) (a) Karle, I. L.; Flippen-Anderson, J. L.; Uma, K.; Balam, P. *Proteins* **1990**, *7*, 62–73. (b) Karle, I. L.; Flippen-Anderson, J.; Uma, K.; Balam, P. *Proc. Natl. Acad. Sci. U.S.A.* **1988**, *85*, 299–303.
- (19) Reinert, Z. E.; Lengyel, G. A.; Horne, W. S. *J. Am. Chem. Soc.* **2013**, *135*, 12528–12531.